

Degeneracy between θ_{23} octant and neutrino non-standard interactions at DUNE

Sanjib Kumar Agarwalla^a, Sabya Sachi Chatterjee^a, Antonio Palazzo^{b,c}

^a*Institute of Physics, Sachivalaya Marg, Sainik School Post, Bhubaneswar 751005, India*

^b*Dipartimento Interateneo di Fisica “Michelangelo Merlin”, Università di Bari, Via G. Amendola 173, I-70126 Bari, Italy*

^c*Istituto Nazionale di Fisica Nucleare, Sezione di Bari, Via Orabona 4, 70126 Bari, Italy*

Abstract

We expound in detail the degeneracy between the octant of θ_{23} and flavor-changing neutral-current non-standard interactions (NSI's) in neutrino propagation, considering the Deep Underground Neutrino Experiment (DUNE) as a case study. In the presence of such NSI parameters involving the $e - \mu$ ($\varepsilon_{e\mu}$) and $e - \tau$ ($\varepsilon_{e\tau}$) flavors, the $\nu_\mu \rightarrow \nu_e$ and $\bar{\nu}_\mu \rightarrow \bar{\nu}_e$ appearance probabilities in long-baseline experiments acquire an additional interference term, which depends on one new dynamical CP-phase $\phi_{e\mu/e\tau}$. This term sums up with the well-known interference term related to the standard CP-phase δ creating a source of confusion in the determination of the octant of θ_{23} . We show that for values of the NSI coupling (taken one at-a-time) as small as *few* % (relative to the Fermi coupling constant G_F), and for unfavorable combinations of the two CP-phases δ and $\phi_{e\mu/e\tau}$, the discovery potential of the octant of θ_{23} gets completely lost.

Keywords: Neutrino, θ_{23} octant, CP-phase, Non-Standard Interactions, Long-baseline, DUNE

1. Introduction

Although the interactions of neutrinos are well described by the Standard Model (SM) of particle physics, it is possible that these particles may participate to new non-standard interactions (NSI's), whose effects are beyond the reach of the existing experiments. NSI's may appear as a low-energy manifestation of high-energy physics involving new heavy states (for a review see [1, 2, 3]) or, alternatively, they can be related to new light mediators [4, 5]. As first recognized in [6], NSI's can profoundly modify the MSW dynamics [6, 7, 8] of the neutrino flavor conversion in matter. As a consequence, they can be a source of confusion in the determination of the standard parameters regulating the 3-flavor oscillations if the estimate of these last ones is extracted from experiments sensitive to MSW effects. Recently, in the context of long-baseline (LBL) experiments, the potential confusion between the standard

Email addresses: sanjib@iopb.res.in (Sanjib Kumar Agarwalla), sabya@iopb.res.in (Sabya Sachi Chatterjee), palazzo@ba.infn.it (Antonio Palazzo)

CP-violation (CPV) related to the 3-flavor CP-phase δ and the dynamical CP-phases implied by neutral-current flavor-changing NSI's has received much attention [9, 10, 11, 12, 13, 14, 15, 16, 17]¹.

In this paper, we explore in detail, a different kind of degeneracy affecting LBL experiments. It is still induced by the new CP-phases related to NSI's, but concerns the octant of the atmospheric mixing angle θ_{23} . Such a degeneracy has been noted in the numerical simulations performed in [21, 22, 23] and also briefly discussed at the analytical level in [11] (see also [9, 16]). But, to the best of our knowledge, it has not been addressed in a systematic way in the literature. We recall that present global neutrino data [24, 25, 26] indicate that θ_{23} may be non-maximal with two degenerate solutions: one $< \pi/4$, dubbed as lower octant (LO), and the other $> \pi/4$, termed as higher octant (HO). Just a few days ago, at the Neutrino 2016 Conference, the NOvA collaboration has reinforced the case of two degenerate solutions, excluding maximal mixing at the 2.5σ confidence level [27]. This makes the octant issue even more pressing than before. The identification of the θ_{23} octant is an important target in neutrino physics, due to the profound implications for the theory of neutrino masses and mixing (see [28, 29, 30, 31, 32] for reviews). In the presence of flavor-changing NSI's involving the $e - \mu$ or $e - \tau$ sectors, the $\nu_\mu \rightarrow \nu_e$ transition probability probed at LBL facilities acquires a new interference term that depends on one new dynamical CP-phase ϕ . This term sums up with the well-known interference term related to the standard CP-phase δ creating a potential source of confusion in the reconstruction of the θ_{23} octant. Taking the Deep Underground Neutrino Experiment (DUNE) [33, 34, 35, 36, 37] as a case study,² we show that for values of the NSI coupling as small as *few %* (relative to the Fermi constant G_F), for unfavorable combinations of the two CP-phases δ and ϕ , the discovery potential of the octant of θ_{23} gets completely lost.

2. Theoretical framework

A neutral-current NSI can be described by a four-fermion dimension-six operator [6]

$$\mathcal{L}_{\text{NC-NSI}} = -2\sqrt{2}G_F \varepsilon_{\alpha\beta}^{fC} (\bar{\nu}_\alpha \gamma^\mu P_L \nu_\beta) (\bar{f} \gamma_\mu P_C f), \quad (1)$$

where subscripts $\alpha, \beta = e, \mu, \tau$ indicate the neutrino flavor, superscript $f = e, u, d$ labels the matter fermions, superscript $C = L, R$ denotes the chirality of the ff current, and $\varepsilon_{\alpha\beta}^{fC}$ are dimensionless quantities which parametrize the

¹Another notable degeneracy occurs between off-diagonal NSI's and non-zero θ_{13} in long-baseline [18] and solar neutrino experiments [19, 20]. Now, this degeneracy has been resolved with the help of data from reactor experiments (Daya Bay, Double Chooz, and RENO), which confirmed that θ_{13} is non-zero without having any dependency on matter effects.

²Recent work on the impact of NSI's at DUNE can be found in [23, 21, 22, 15, 17, 38].

strengths of the NSI's. The hermiticity of the interaction demands

$$\varepsilon_{\beta\alpha}^{fC} = (\varepsilon_{\alpha\beta}^{fC})^* . \quad (2)$$

For neutrino propagation through matter, the relevant combinations are

$$\varepsilon_{\alpha\beta} \equiv \sum_{f=e,u,d} \varepsilon_{\alpha\beta}^f \frac{N_f}{N_e} \equiv \sum_{f=e,u,d} (\varepsilon_{\alpha\beta}^{fL} + \varepsilon_{\alpha\beta}^{fR}) \frac{N_f}{N_e} , \quad (3)$$

where N_f denotes the number density of fermion f . For the Earth, we can assume neutral and isoscalar matter, implying $N_n \simeq N_p = N_e$, in which case $N_u \simeq N_d \simeq 3N_e$. Therefore,

$$\varepsilon_{\alpha\beta} \simeq \varepsilon_{\alpha\beta}^e + 3\varepsilon_{\alpha\beta}^\mu + 3\varepsilon_{\alpha\beta}^d . \quad (4)$$

The NSI's modify the effective Hamiltonian for neutrino propagation in matter, which in the flavor basis reads

$$H = U \begin{bmatrix} 0 & 0 & 0 \\ 0 & k_{21} & 0 \\ 0 & 0 & k_{31} \end{bmatrix} U^\dagger + V_{\text{CC}} \begin{bmatrix} 1 + \varepsilon_{ee} & \varepsilon_{e\mu} & \varepsilon_{e\tau} \\ \varepsilon_{e\mu}^* & \varepsilon_{\mu\mu} & \varepsilon_{\mu\tau} \\ \varepsilon_{e\tau}^* & \varepsilon_{\mu\tau}^* & \varepsilon_{\tau\tau} \end{bmatrix} , \quad (5)$$

where U is the Pontecorvo-Maki-Nakagawa-Sakata (PMNS) matrix, which, in the standard parameterization, depends on three mixing angles ($\theta_{12}, \theta_{13}, \theta_{23}$) and one CP-phase (δ). We have also introduced the solar and atmospheric wavenumbers $k_{21} \equiv \Delta m_{21}^2/2E$ and $k_{31} \equiv \Delta m_{31}^2/2E$ and the charged-current matter potential

$$V_{\text{CC}} = \sqrt{2}G_F N_e \simeq 7.6 Y_e \times 10^{-14} \left[\frac{\rho}{\text{g/cm}^3} \right] \text{eV} , \quad (6)$$

where $Y_e = N_e/(N_p + N_n) \simeq 0.5$ is the relative electron number density in the Earth crust. It is useful to introduce the dimensionless quantity $v = V_{\text{CC}}/k_{31}$, whose absolute value is given by

$$|v| = \left| \frac{V_{\text{CC}}}{k_{31}} \right| \simeq 0.22 \left[\frac{E}{2.5 \text{ GeV}} \right] , \quad (7)$$

since it will appear in the analytical expressions of the $\nu_\mu \rightarrow \nu_e$ transition probability. In Eq. (7), we have taken the energy of the DUNE first oscillation maximum $E = 2.5 \text{ GeV}$ as a benchmark.

In the present work, we limit our investigation to flavor non-diagonal NSI's, that is, we only allow the $\varepsilon_{\alpha\beta}$'s with

$\alpha \neq \beta$ to be non-zero. More specifically, we will focus our attention on the couplings $\varepsilon_{e\mu}$ and $\varepsilon_{e\tau}$, which, as will we discuss in detail, introduce an observable dependency from their associated CP-phase in the appearance $\nu_\mu \rightarrow \nu_e$ probability probed at the LBL facilities. For completeness, we will comment about the (different) role of the third coupling $\varepsilon_{\mu\tau}$, which mostly affects the $\nu_\mu \rightarrow \nu_\mu$ disappearance channel and has not a critical impact in the θ_{23} octant reconstruction. We recall that the current upper bounds (at 90% C.L.) on the two NSI's under consideration are: $|\varepsilon_{e\mu}| \lesssim 0.33$, as reported in the review [1], and $|\varepsilon_{e\tau}| \lesssim 0.45$ as derived from the most recent Super-Kamiokande atmospheric data analysis [39] under the assumption $\varepsilon_{ee} = 0$ (see also [40]). As we will show in detail, the strengths of $|\varepsilon_{e\mu}|$ and $|\varepsilon_{e\tau}|$ that can give rise to a degeneracy problem with the octant of θ_{23} are one order of magnitude smaller than these upper bounds.

3. Analytical Expressions

Let us consider the transition probability relevant for the LBL experiment DUNE. Using the expansions available in the literature [41] one can see that in the presence of a NSI, the transition probability can be written approximately as the sum of three terms

$$P_{\mu e} \simeq P_0 + P_1 + P_2, \quad (8)$$

where the first two terms return the standard 3-flavor probability and the third one is ascribed to the presence of NSI. Noting that the small mixing angle $\sin \theta_{13}$, the matter parameter v and the modulus $|\varepsilon|$ of the NSI can be considered approximately of the same order of magnitude $O(\varepsilon)$, while $\alpha \equiv \Delta m_{21}^2 / \Delta m_{31}^2 = \pm 0.03$ is $O(\varepsilon^2)$, one can expand the probability keeping only third order terms. Using a notation similar to that adopted in [11], we obtain³

$$P_0 \simeq 4s_{13}^2 s_{23}^2 f^2, \quad (9)$$

$$P_1 \simeq 8s_{13}s_{12}c_{12}s_{23}c_{23}\alpha f g \cos(\Delta + \delta), \quad (10)$$

$$P_2 \simeq 8s_{13}s_{23}v|\varepsilon|[af^2 \cos(\delta + \phi) + bfg \cos(\Delta + \delta + \phi)], \quad (11)$$

³Interestingly, a similar decomposition of the transition probability is valid in the presence of a light sterile neutrino [42]. In that case, however, the origin of the new interference term P_2 is kinematical, and it is operative also in vacuum. In fact, the new term is related to the interference of the atmospheric oscillations with those induced by the new large mass-squared splitting implied by the sterile state.

where $\Delta \equiv \Delta m_{31}^2 L/4E$ is the atmospheric oscillating frequency related to the baseline L . For compactness, we have used the notation ($s_{ij} \equiv \sin \theta_{ij}$, $c_{ij} \equiv \cos \theta_{ij}$), and following [43], we have introduced the quantities

$$f \equiv \frac{\sin[(1-\nu)\Delta]}{1-\nu}, \quad g \equiv \frac{\sin \nu \Delta}{\nu}. \quad (12)$$

We observe that P_0 is positive definite being independent of the CP-phases, and gives the leading contribution to the probability. In P_1 one recognizes the standard 3-flavor interference term between the solar and the atmospheric frequencies. The third term P_2 brings the dependency on the (complex) NSI coupling and of course is non-zero only in the presence of matter (i.e. if $\nu \neq 0$). In Eq. (11) we have assumed for the NSI coupling the general complex form

$$\varepsilon = |\varepsilon| e^{i\phi}. \quad (13)$$

The expression of P_2 is slightly different for $\varepsilon_{e\mu}$ and $\varepsilon_{e\tau}$ and, in Eq. (11), one has to put

$$a = s_{23}^2, \quad b = c_{23}^2 \quad \text{if} \quad \varepsilon = |\varepsilon_{e\mu}| e^{i\phi_{e\mu}}, \quad (14)$$

$$a = s_{23}c_{23}, \quad b = -s_{23}c_{23} \quad \text{if} \quad \varepsilon = |\varepsilon_{e\tau}| e^{i\phi_{e\tau}}. \quad (15)$$

In the expressions given above for P_0 , P_1 and P_2 , one should bear in mind that the sign of Δ , α and ν is positive (negative) for NH (IH). In addition, we stress that the expressions above are valid for neutrinos, and that the corresponding ones for antineutrinos are obtained by inverting the sign of all the CP-phases, and of the dimensionless quantity ν .

Now let us come to the θ_{23} octant issue. As a first step it is useful to quantify the size of the perturbation from maximal mixing allowed by current data. We can express the atmospheric mixing angle as

$$\theta_{23} = \frac{\pi}{4} \pm \eta, \quad (16)$$

where η is a positive-definite angle. The positive (negative) sign corresponds to HO (LO). The current 3-flavor global analyses [24, 25, 26] indicate that θ_{23} cannot deviate from 45° by more than $\sim 6^\circ$, i.e. s_{23}^2 must be in the range $\sim [0.4, 0.6]$. Therefore, one has $\eta \lesssim 0.1$, and we can use the expansion

$$s_{23}^2 = \frac{1}{2}(1 \pm \sin 2\eta) \simeq \frac{1}{2} \pm \eta. \quad (17)$$

An experiment is sensitive to the octant if, in spite of the freedom provided by the unknown CP-phases, there is still a

non-zero difference among the transition probability in the two octants, i.e.

$$\Delta P \equiv P_{\mu e}^{\text{HO}}(\theta_{23}^{\text{HO}}, \delta^{\text{HO}}, \phi^{\text{HO}}) - P_{\mu e}^{\text{LO}}(\theta_{23}^{\text{LO}}, \delta^{\text{LO}}, \phi^{\text{LO}}) \neq 0. \quad (18)$$

In Eq. (18) one of the two octants should be thought as the true octant (whose value is used to simulate the data) and the other one as the test one (whose value is used to simulate the theoretical model). For example, if for definiteness we fix the HO as the true octant, then for a given combination of $(\delta_{\text{true}}^{\text{HO}}, \phi_{\text{true}}^{\text{HO}})$ there is sensitivity to the octant if there exist some values of the test phases $(\delta_{\text{test}}^{\text{LO}}, \phi_{\text{test}}^{\text{LO}})$ such that $\Delta P \neq 0$ at a detectable level⁴.

According to Eq. (8), we can split ΔP in the sum of three terms

$$\Delta P = \Delta P_0 + \Delta P_1 + \Delta P_2. \quad (19)$$

The first term is positive-definite, does not depend on the CP-phases and, at the first order in η , it is given by

$$\Delta P_0 \simeq 8\eta s_{13}^2 f^2. \quad (20)$$

The second and third terms depend on the CP-phases and can have both positive or negative values. Their expressions are given by

$$\Delta P_1 = A[\cos(\Delta + \delta^{\text{HO}}) - \cos(\Delta + \delta^{\text{LO}})], \quad (21)$$

$$\Delta P_2 = B[\cos(\delta^{\text{HO}} + \phi^{\text{HO}}) - \cos(\delta^{\text{LO}} + \phi^{\text{LO}})] \pm C[\cos(\Delta + \delta^{\text{HO}} + \phi^{\text{HO}}) - \cos(\Delta + \delta^{\text{LO}} + \phi^{\text{LO}})], \quad (22)$$

where for compactness, we have introduced the amplitudes⁵

$$A = 4s_{13}s_{12}c_{12}\alpha f g, \quad (23)$$

$$B = 2\sqrt{2}\nu|\varepsilon|s_{13}f^2, \quad (24)$$

$$C = 2\sqrt{2}\nu|\varepsilon|s_{13}f g. \quad (25)$$

The positive (negative) sign in front of the coefficient C in Eq. (22) corresponds to $\varepsilon_{e\mu}$ ($\varepsilon_{e\tau}$). In order to get a feeling of the size of the three terms of ΔP we provide a ballpark estimate adopting as a benchmark case (ν , NH), and fixing the energy at the value $E = 2.5$ GeV corresponding to the first oscillation maximum ($\Delta = \pi/2$), in which case

⁴In the numerical analysis the values of the test parameters are determined by minimization of the $\Delta\chi^2$ [see Eq. (29) in Section 4].

⁵In the expressions of A , B and C we are neglecting terms proportional to powers of η , which would give rise to negligible corrections.

$|f| = |\sin \Delta| = 1$ and $|g| = |\Delta| = \pi/2$. For the 3-flavor parameters, we have used the values provided at the beginning of the next section. For the first term we find

$$\Delta P_0 \simeq 1.26 \times 10^{-2} \left[\frac{\eta}{0.05} \right], \quad (26)$$

where we have left manifest the linear dependency on the deviation η from maximal θ_{23} . The amplitude of the standard interference term ΔP_1 is

$$|A| \simeq 1.52 \times 10^{-2}, \quad (27)$$

while, for the two coefficients entering the NSI-induced term ΔP_2 , one finds

$$|B| + |C| \simeq 1.51 \times 10^{-2} \left[\frac{|\varepsilon|}{0.05} \right], \quad (28)$$

where we have left evident the linear dependency on the NSI strength $|\varepsilon|$. From this last relation we see that for values of the NSI coupling $|\varepsilon| \sim 0.05$, the difference induced by the new interference term (ΔP_2) has approximately the same amplitude of that arising from the standard interference term (ΔP_1). Also, it is essential to notice that the third term ΔP_2 in Eq. (22) depends not only on the standard CP-phase δ but also on the new dynamical CP-phase ϕ related to the NSI. Since the two CP-phases δ and ϕ are independent quantities, in the SM+NSI scheme there is much more freedom with respect to the SM case, where only one phase (δ) is present. Therefore, for sufficiently large values of the NSI coupling, it is reasonable to expect a degradation of the reconstruction of the θ_{23} octant, which will depend on the amplitude of the deviation η .

Figure 1 provides a useful geometrical representation of the situation. In such a plot, the ellipses refer to the SM case, while the colored blobs represent the SM+NSI scheme. In each panel we show the four cases corresponding to the different choice of the neutrino mass hierarchy (MH), which can be normal (NH) or inverted (IH), and to the different choice of the octant (LO and HO). We have taken $\sin^2 \theta_{23} = 0.42$ (0.58) as a benchmark value for the LO (HO) octant. In the left (right) panel we have switched on the $e\mu$ ($e\tau$) coupling taking for its modulus $|\varepsilon_{e\mu}| = 0.05$ ($|\varepsilon_{e\tau}| = 0.05$) and varying the associated CP-phase $\phi_{e\mu}$ ($\phi_{e\tau}$) in its allowed interval $[-\pi, \pi]$. The graphs neatly show that the θ_{23} octant separation existing in the SM case is lost in the presence of NSI's since the two separate ellipses become overlapping blobs. We can understand how the blobs arise thinking them as a convolution of an infinite ensemble of ellipses (for more examples, see [44, 45]), each corresponding to a different value of the new phase ($\phi_{e\mu}$ or $\phi_{e\tau}$). The orientation of the ellipses changes as a function of such new CP-phase covering a full area in the bi-event space.

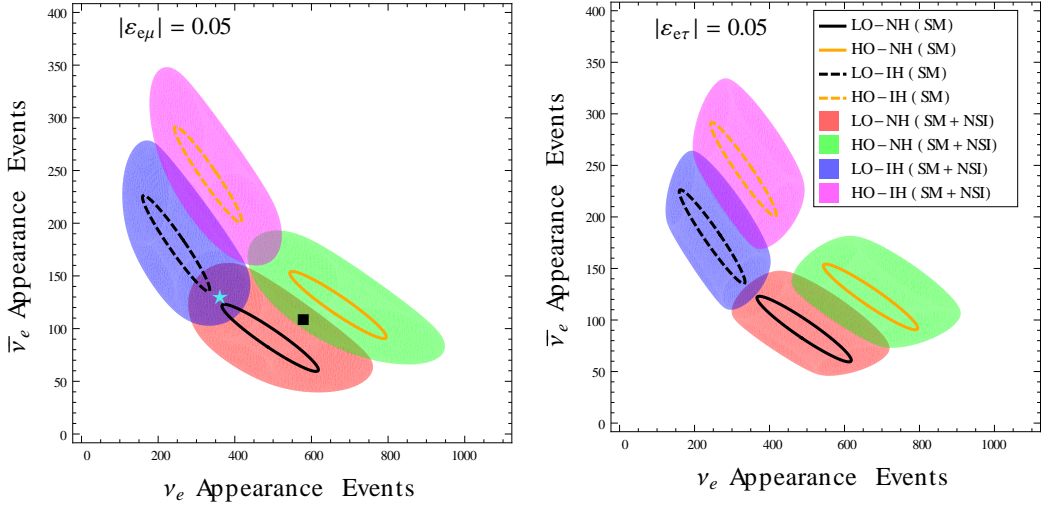


Figure 1: Bi-event plot for the DUNE setup. The ellipses represent the SM case, while the colored blobs correspond to SM+NSI (see the legends). We take $\sin^2 \theta_{23} = 0.42$ (0.58) as benchmark value for the LO (HO). In the SM ellipses, the running parameter is δ varying in the range $[-\pi, \pi]$. In case of SM+NSI blobs, there are two running parameters: δ and $\phi_{e\mu}$ (δ and $\phi_{e\tau}$) in the left (right) panel, both varying in their allowed ranges $[-\pi, \pi]$.

The shape of the colored blobs is slightly different between the two cases of $\varepsilon_{e\mu}$ and $\varepsilon_{e\tau}$ as a result of the different functional dependency of the transition probability. One can notice that in both panels there is also an overlap among the two hierarchies, which is more pronounced in the $e\mu$ case (left panel) if compared with the $e\tau$ case (right panel). This may indicate that the MH may be a source of degeneracy in the octant identification.

This is not the case, however, because in the DUNE experiment the energy spectrum brings additional information that breaks the MH degeneracy. In contrast, the energy spectrum is not able to offer much help in lifting the octant degeneracy. This behavior is elucidated by Fig. 2, which represents the reconstructed electron neutrino event spectra in DUNE for $|\varepsilon_{e\mu}| = 0.05$ plotted for four representative cases. The left panel illustrates the comparison of two cases in which the total number of ν_e events is exactly the same for NH and IH. The right panel displays the comparison of two cases in which the total number of events is exactly the same for LO and HO. The two spectra on the left panel are calculated for the values of the CP-phases δ and $\phi_{e\mu}$ indicated in the legend, which correspond to the same point in the bievent space located in the overlapping region of the two (red and blue) LO blobs (the cyan star in the left panel of Fig. 1). The two spectra on the right panel are calculated for the values of the CP-phases δ and $\phi_{e\mu}$ indicated in the legend, which correspond to the same point in the bievent space located in the overlapping region of the two (red and green) NH blobs (the black square in the left panel of Fig. 1). Figure 2 clearly shows that, while the spectra are rather different for the two hierarchies, especially at low energies, they are almost identical for the two octants. We find a similar behavior in the electron antineutrino spectra (not shown) for the same choices of the CP-phases indicated in

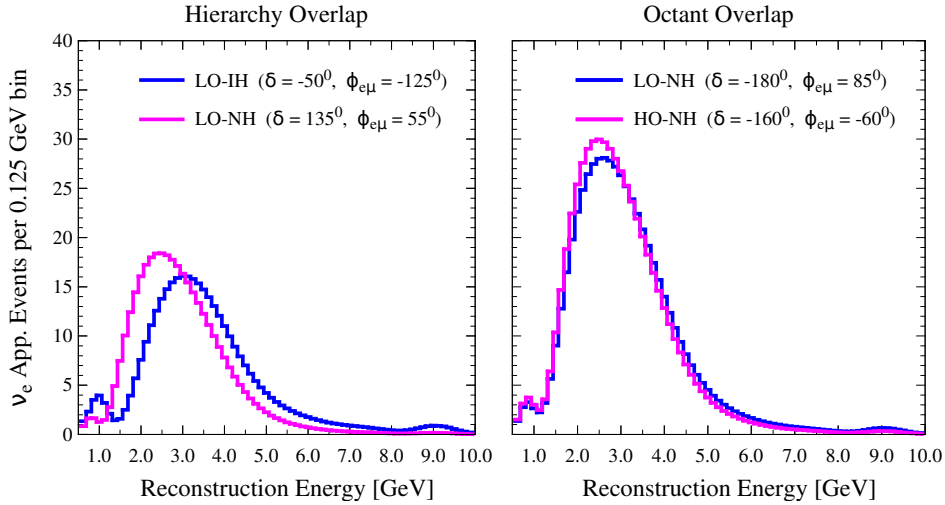


Figure 2: Electron neutrino spectra of DUNE for $|\varepsilon_{e\mu}| = 0.05$ plotted for four representative cases. The left panel illustrates the comparison of two cases in which the total number of events is exactly the same for NH and IH (corresponding to the cyan star in the left panel of Fig. 1). The right panel displays the comparison of two cases in which the total number of events is exactly the same for LO and HO (corresponding to the black square in the left panel of Fig. 1). See the text for more details.

the legend of Fig. 2. This implies that the MH is not a source of confusion in the octant identification⁶. Nonetheless, for generality, in the numerical analysis presented in the next section, we will treat the MH as an unknown parameter.

4. Numerical results

For DUNE, we consider a 35 kiloton fiducial liquid argon far detector in our work, and follow the detector characteristics which are mentioned in Table 1 of Ref. [47]. We assume a proton beam power of 708 kW in its initial phase with a proton energy of 120 GeV which can deliver 6×10^{20} protons on target in 230 days per calendar year. In our calculation, we have used the fluxes which were obtained assuming a decay pipe length of 200 m and 200 kA horn current [48]. We take a total run time of ten years, which is equivalent to a total exposure of 248 kiloton · MW · year, equally shared between neutrino and antineutrino modes. In our work, we consider the reconstructed energy range of neutrino and antineutrino to be 0.5 GeV to 10 GeV. As far as the systematic uncertainties are concerned, we assume an uncorrelated 5% normalization error on signal, and 5% normalization error on background for both the appearance and disappearance channels. The same set of systematics are taken for both the neutrino and antineutrino channels which are also uncorrelated. In our simulations, we use the GLoBES software [49, 50]. We incorporate the effect of the NSI parameters both in the $\nu_\mu \rightarrow \nu_e$ appearance channel, and in the $\nu_\mu \rightarrow \nu_\mu$ disappearance channel. The same is also applicable for the antineutrino run. The benchmark (central) values of the three-flavor oscillation

⁶In [11, 46], it has been pointed out that if ε_{ee} is non-zero and $\mathcal{O}(1)$, then DUNE alone cannot determine the correct MH. In such a scenario, the octant ambiguity that we are dealing with can be further exacerbated.

parameters that we consider in this work are: $\sin^2 \theta_{12} = 0.304$, $\sin^2 2\theta_{13} = 0.085$, $\sin^2 \theta_{23} = 0.42$ (0.58) for LO (HO), $\Delta m_{21}^2 = 7.50 \times 10^{-5}$ eV 2 , Δm_{31}^2 (NH) = 2.475×10^{-3} eV 2 , Δm_{31}^2 (IH) = -2.4×10^{-3} eV 2 , and the CP phase δ in the range $[-\pi, \pi]$. These choices of the oscillation parameters are in close agreement with the recent best-fit values from Ref. [24, 25, 26]. For the cases, where the results are shown as a function of true value of $\sin^2 \theta_{23}$, we consider the 3σ allowed range of 0.38 to 0.63. For the DUNE baseline of 1300 km, we take the line-averaged constant Earth matter density of $\rho = 2.87$ g/cm 3 estimated using the Preliminary Reference Earth Model (PREM) [51]. To obtain the numerical results, we carry out a full spectral analysis using the binned events spectra for DUNE. In order to determine the sensitivity of DUNE for excluding the false octant, we define the Poissonian $\Delta\chi^2$ as

$$\Delta\chi^2 = \chi^2_{\text{false octant}} - \chi^2_{\text{true octant}}, \quad (29)$$

where $\chi^2_{\text{true octant}}$ ($\chi^2_{\text{false octant}}$) is generated for the true (test) values of $(\theta_{23}, \delta, \phi)$. To obtain the curves displayed in Fig. 3, for any given choice of the true parameters, we minimize the $\Delta\chi^2$ in Eq. (29) with respect to the test parameters varying $\theta_{23}^{\text{test}}$ in the false octant and $(\delta^{\text{test}}, \phi^{\text{test}})$ in the range $[-\pi, \pi]$. In addition, in Fig. 4 we marginalize also over ϕ^{true} in the range $[-\pi, \pi]$. Finally, in Fig. 5 we also marginalize over δ^{true} . We follow the method of pulls as described in Refs. [52, 53] to marginalize $\Delta\chi^2$ over the uncorrelated systematic uncertainties. To give our results at 1, 2, 3σ confidence levels for 1 d.o.f., we use the relation $N\sigma \equiv \sqrt{\Delta\chi^2}$, which is valid in the frequentist method of hypothesis testing [54].

Figure 3 displays the sensitivity for excluding the wrong octant as a function of true δ . The two upper panels refer to $\varepsilon_{e\mu}$ while the two lower panels refer to $\varepsilon_{e\tau}$. In each case we fix the modulus of the coupling ($|\varepsilon_{e\mu}|$ or $|\varepsilon_{e\tau}|$) equal to 0.05. The two left (right) panels refer to the true choice LO-NH (HO-NH). In all panels, for the sake of comparison, we show the results for the 3-flavor SM case (represented by the black curve). Concerning the SM+NSI scheme, we draw the curves corresponding to four representative values of the (true) dynamical CP-phase ($\phi_{e\mu}$ or $\phi_{e\tau}$). In the SM case we have marginalized over (θ_{23}, δ) (test). In the SM+NSI scheme, we have also marginalized over the test value of the new dynamical CP-phase ($\phi_{e\mu}$ or $\phi_{e\tau}$). In all cases we have marginalized over the mass hierarchy. However, we have checked that the minimum of $\Delta\chi^2$ is never reached in the wrong hierarchy. This confirms that the neutrino mass hierarchy is not an issue in the determination of the θ_{23} octant in DUNE, as expected on the basis of the discussion about the energy spectral information made in the previous section.

In the analysis shown in Fig 3, we have fixed $\sin^2 \theta_{23} = 0.42$ (0.58) as a benchmark value for the LO (HO), corresponding to a deviation $\eta = \pm 0.08$. In general, one may want to know how things change for different choices of the true value of θ_{23} since it is unknown. Figure 4 gives a quantitative answer to this question. It displays the discovery

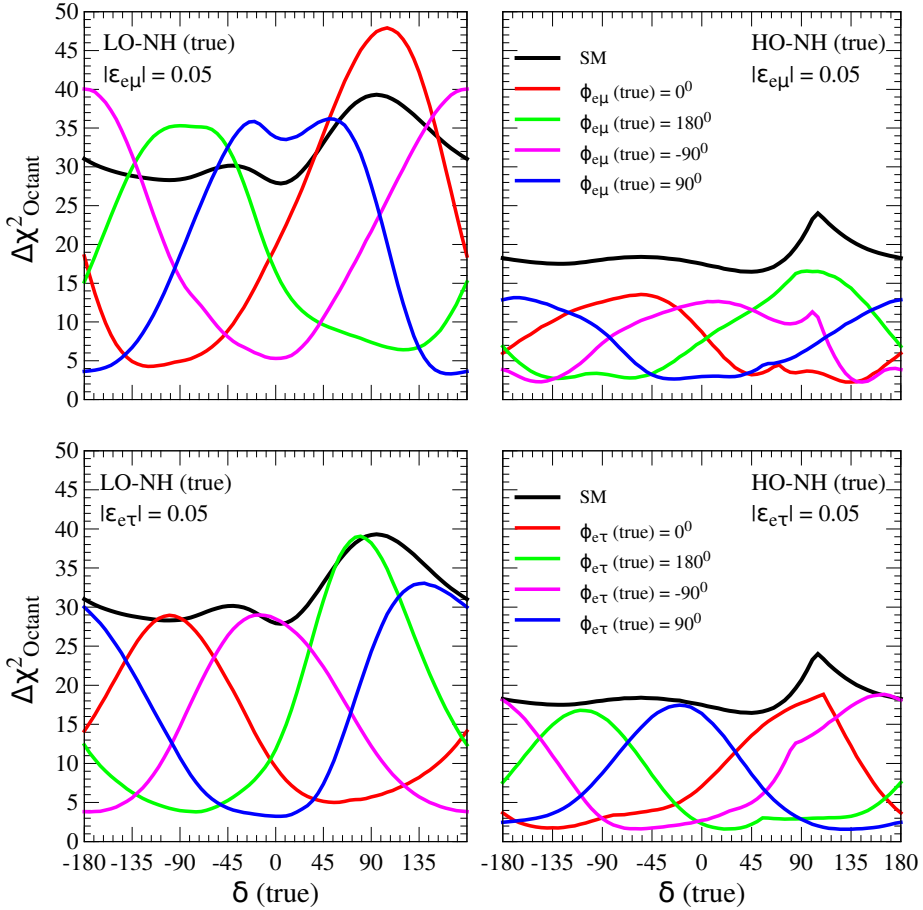


Figure 3: Discovery potential of the true octant as a function of true δ assuming LO-NH (left panels) and HO-NH (right panels) as the true choice. We take $\sin^2 \theta_{23} = 0.42$ (0.58) as benchmark value for the LO (HO). In each panel, we present the results for the SM case (black line), and for the SM+NSI scheme (colored lines) considering four different values of true $\phi_{e\mu}$ (upper panels) and $\phi_{e\tau}$ (lower panels). In the SM case, we marginalize away (θ_{23}, δ) (test). In the SM+NSI scheme, we fix $|\varepsilon_{e\mu}| = 0.05$ in the two upper panels and $|\varepsilon_{e\tau}| = 0.05$ in the two lower panels. In the two upper panels, we marginalize over $(\theta_{23}, \delta, \phi_{e\mu})$ (test), while in the two lower ones, we marginalize over $(\theta_{23}, \delta, \phi_{e\tau})$ (test).

potential of the true octant in the $[\sin^2 \theta_{23}, \delta]$ (true) plane, assuming NH as true choice. The left panel corresponds to the SM case. The middle (right) panel represents the SM+NSI case, where we have “switched on” $\varepsilon_{e\mu}$ ($\varepsilon_{e\tau}$) with modulus 0.05. In the SM case we have marginalized away (θ_{23}, δ) (test). In the SM+NSI cases, in addition, we have marginalized over the true and test value of the new dynamical CP-phase ($\phi_{e\mu}$ in the middle panel, $\phi_{e\tau}$ in the right panel). The solid blue, dashed magenta, and dotted black curves correspond, respectively, to the 2σ , 3σ , and 4σ confidence levels (1 d.o.f.). From the comparison of the middle and right panels with the left one, we can see that the presence of NSI with strength $|\varepsilon| = 0.05$ compromises the octant sensitivity for all the phenomenologically interesting region allowed for s_{23}^2 by current data. This is of particular interest because such low strengths of the NSI’s are well below the current upper bounds both for $\varepsilon_{e\mu}$ and $\varepsilon_{e\tau}$. Finally, it is interesting to ask how the deterioration of the θ_{23} octant discovery potential varies with the NSI strength. For this purpose one needs to treat the NSI strength as a free

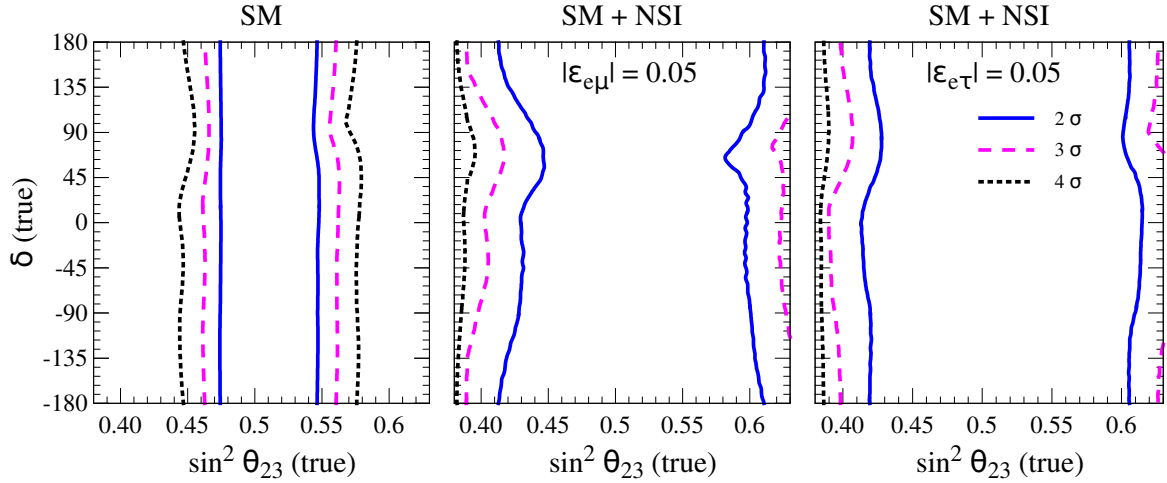


Figure 4: Discovery potential of the true octant in $[\sin^2 \theta_{23}, \delta]$ (true) plane assuming NH as true choice. The left panel corresponds to the SM case. The middle (right) panel represents the SM+NSI case where we have switched on $\epsilon_{e\mu}$ ($\epsilon_{e\tau}$). In the SM case, we marginalize away (θ_{23}, δ) (test). In the SM+NSI cases, in addition, we marginalize over the true and test value of the additional CP-phase ($\phi_{e\mu}$ in the middle panel, $\phi_{e\tau}$ in the right panel). The solid blue, dashed magenta, and dotted black curves correspond, respectively, to the 2σ , 3σ , and 4σ confidence levels (1 d.o.f.).

parameter, allowing the associated CP-phase to vary in the interval $[-\pi, \pi]$. The results of this general analysis are represented in Fig 5, which shows the discovery potential of the θ_{23} octant in the plane $[\lvert \epsilon \rvert, \sin^2 \theta_{23}]$ (true), assuming NH as true choice. The left (right) panel corresponds to $\epsilon \equiv \epsilon_{e\mu}$ ($\epsilon \equiv \epsilon_{e\tau}$). In both cases, the standard parameters (θ_{23}, δ) (test) and δ (true) have been marginalized away. In addition, in the left (right) panel the true and test values of the CP-phase $\phi_{e\mu}$ ($\phi_{e\tau}$) have been marginalized away. We observe that for NSI strengths below the 1% level, the sensitivity substantially coincides with that achieved in the SM case. In this case the NSI's are harmless. For larger values, the sensitivity gradually deteriorates, until it basically goes below the 2σ level for all the interesting values of $\sin^2 \theta_{23}$ if $\lvert \epsilon \rvert \gtrsim 0.07$.

Before concluding this section, a remark is in order concerning the off-diagonal coupling $\epsilon_{\mu\tau}$. First, one should note that this coupling is the most strongly constrained due to the high sensitivity of atmospheric neutrino data to the $\nu_\mu \rightarrow \nu_\tau$ transitions. The most recent Super-Kamiokande analysis provides the upper bound $\lvert \epsilon_{\mu\tau} \rvert \lesssim 0.033$ at the 90% C.L. [39] (see also [55]), whose results are corroborated by MINOS data [56]. Second, in the context of long-baseline experiments, $\epsilon_{\mu\tau}$ essentially affects only the $\nu_\mu \rightarrow \nu_\mu$ disappearance probability, while its effects on the $\nu_\mu \rightarrow \nu_e$ appearance probability are negligible. These two circumstances make the $\epsilon_{\mu\tau}$ coupling less important for what concerns the discrimination of the octant of θ_{23} . This fact is corroborated by our numerical simulations. We have explicitly verified that even for $\lvert \epsilon_{\mu\tau} \rvert = 0.05$, which is well above the present upper bound, the DUNE sensitivity to the octant of θ_{23} never goes below 4.4σ (3.1σ) for the benchmark value $s_{23}^2 = 0.42$ (0.58) for LO (HO). Also, we find only mild changes in the sensitivity when the associated CP-phase $\phi_{\mu\tau}$ is allowed to vary in the interval $[-\pi, \pi]$.

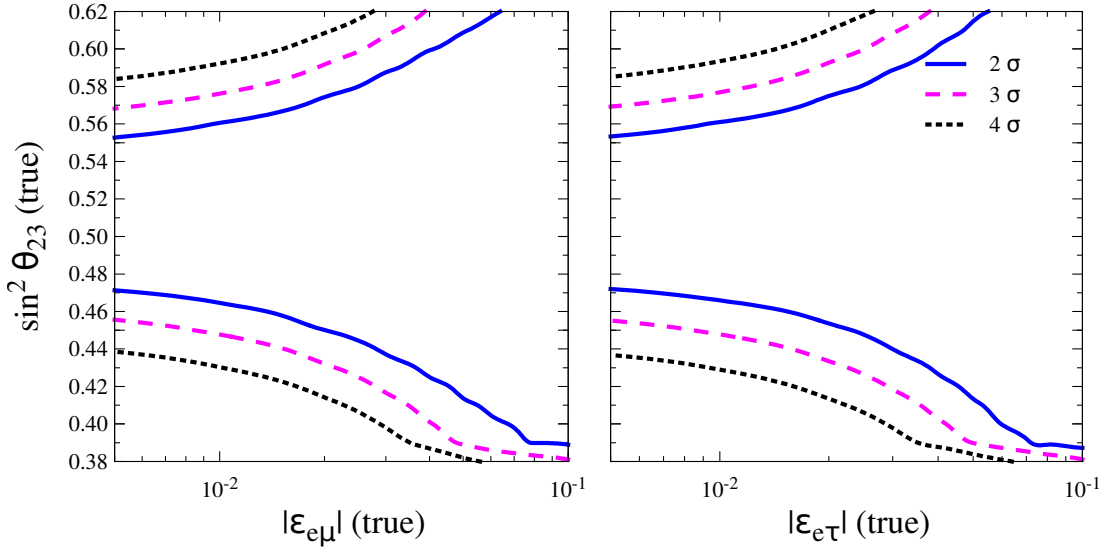


Figure 5: Degradation of the θ_{23} octant sensitivity as a function of the NSI strength $|\varepsilon|$, assuming NH as true choice. The left (right) panel corresponds to $\varepsilon \equiv \varepsilon_{e\mu}$ ($\varepsilon \equiv \varepsilon_{e\tau}$). In both cases, θ_{23} (test) and δ (both true and test) have been marginalized away. In addition, in the left (right) panel, the true and test values of the CP-phase $\phi_{e\mu}$ ($\phi_{e\tau}$) have been marginalized away. The solid blue, dashed magenta, and dotted black curves correspond, respectively, to the 2σ , 3σ , and 4σ confidence levels (1 d.o.f.).

5. Conclusions

We have investigated the impact of non-standard flavor-changing interactions (NSI) on the reconstruction of the octant of the atmospheric mixing angle θ_{23} in the next generation LBL experiments, taking the Deep Underground Neutrino Experiment (DUNE) as a case study. In the presence of such new interactions the $\nu_\mu \rightarrow \nu_e$ transition probability acquires an additional interference term, which depends on one new dynamical CP-phase ϕ . This term sums up with the well-known interference term related to the standard CP-phase δ . For values of the NSI coupling as small as *few %* (relative to the Fermi constant G_F) the combination of the two interference terms can mimic a swap of the θ_{23} octant. As a consequence, for unfavorable values of the two CP-phases δ and ϕ , the discovery potential of the octant of θ_{23} gets completely lost. We point out that the degeneracy between the octant of θ_{23} and NSI's discussed in this paper has now become more important in light of the new results from the NO_νA Collaboration presented a few days ago at the Neutrino 2016 conference, which suggest that maximal θ_{23} is disfavored at the 2.5σ confidence level [27].

We close the paper with a general remark. In a previous work [57], we found that a similar loss of sensitivity to the θ_{23} octant can occur due to the presence of a light eV-scale sterile neutrino. Also in that case a new interference term appears in the $\nu_\mu \rightarrow \nu_e$ transition probability, which depends on one additional CP-phase. Therefore, albeit in the two cases the origin of the new CP-phase is completely different, having kinematical nature in the sterile neutrino case and dynamical nature in the NSI case, their phenomenological manifestation at the far detector of LBL experiments is

very similar. On the basis of this observation, we can predict an analogous behavior also for other mechanisms which involve a new interference term in the transition probability, like for example the violation of unitarity of the PMNS matrix recently investigated in [58]. Therefore, we can conclude that in general, whenever a new interference term due to any new physics crops up in the LBL $\nu_\mu \rightarrow \nu_e$ appearance probability, the reconstruction of the θ_{23} octant may be in danger.

Acknowledgments

S.K.A. is supported by the DST/INSPIRE Research Grant [IFA-PH-12], Department of Science & Technology, India. A.P. is supported by the Grant “Future In Research” *Beyond three neutrino families*, contract no. YVI3ST4, of Regione Puglia, Italy.

References

References

- [1] C. Biggio, M. Blennow, and E. Fernandez-Martinez, “General bounds on non-standard neutrino interactions,” *JHEP* **0908**, 090 (2009), 0907.0097.
- [2] T. Ohlsson, “Status of non-standard neutrino interactions,” *Rept. Prog. Phys.* **76**, 044201 (2013), 1209.2710.
- [3] O. Miranda and H. Nunokawa, “Non standard neutrino interactions,” (2015), 1505.06254.
- [4] Y. Farzan, “A model for large non-standard interactions of neutrinos leading to the LMA-Dark solution,” *Phys. Lett.* **B748**, 311 (2015), 1505.06906.
- [5] Y. Farzan and I. M. Shoemaker, “Lepton Flavor Violating Non-Standard Interactions via Light Mediators,” (2015), 1512.09147.
- [6] L. Wolfenstein, “Neutrino Oscillations in Matter,” *Phys. Rev.* **D17**, 2369 (1978).
- [7] S. Mikheev and A. Y. Smirnov, “Resonance Amplification of Oscillations in Matter and Spectroscopy of Solar Neutrinos,” *Sov.J.Nucl.Phys.* **42**, 913 (1985).
- [8] S. Mikheev and A. Y. Smirnov, “Resonant amplification of neutrino oscillations in matter and solar neutrino spectroscopy,” *Nuovo Cim.* **C9**, 17 (1986).
- [9] A. Friedland and I. M. Shoemaker, “Searching for Novel Neutrino Interactions at NOvA and Beyond in Light of Large θ_{13} ,” (2012), 1207.6642.
- [10] Z. Rahman, A. Dasgupta, and R. Adhikari, “The Discovery reach of CP violation in neutrino oscillation with non-standard interaction effects,” *J.Phys.* **G42**, 065001 (2015), 1503.03248.
- [11] J. Liao, D. Marfatia, and K. Whisnant, “Degeneracies in long-baseline neutrino experiments from nonstandard interactions,” *Phys. Rev.* **D93**, 093016 (2016), 1601.00927.
- [12] D. V. Forero and P. Huber, “Hints for leptonic CP violation or New Physics?,” (2016), 1601.03736.
- [13] K. Huitu, T. J. Kärkkäinen, J. Maalampi, and S. Vihonen, “Constraining the nonstandard interaction parameters in long baseline neutrino experiments,” *Phys. Rev.* **D93**, 053016 (2016), 1601.07730.
- [14] P. Bakhti and Y. Farzan, “CP-Violation and Non-Standard Interactions at the MOMENT,” (2016), 1602.07099.

[15] M. Masud and P. Mehta, “Non-standard interactions spoiling the CP violation sensitivity at DUNE and other long baseline experiments,” (2016), 1603.01380.

[16] C. Soumya and R. Mohanta, “Implications of lepton flavour violation on long baseline neutrino oscillation experiments,” (2016), 1603.02184.

[17] A. de Gouv  a and K. J. Kelly, “False Signals of CP-Invariance Violation at DUNE,” (2016), 1605.09376.

[18] P. Huber, T. Schwetz, and J. Valle, “Confusing nonstandard neutrino interactions with oscillations at a neutrino factory,” *Phys.Rev.* **D66**, 013006 (2002), [hep-ph/0202048](#).

[19] A. Palazzo and J. W. F. Valle, “Confusing non-zero θ_{13} with non-standard interactions in the solar neutrino sector,” *Phys. Rev.* **D80**, 091301 (2009), 0909.1535.

[20] A. Palazzo, “Hint of non-standard dynamics in solar neutrino conversion,” *Phys. Rev.* **D83**, 101701 (2011), 1101.3875.

[21] P. Coloma, “Non-Standard Interactions in propagation at the Deep Underground Neutrino Experiment,” *JHEP* **03**, 016 (2016), 1511.06357.

[22] M. Blennow, S. Choubey, T. Ohlsson, D. Pramanik, and S. K. Raut, “A combined study of source, detector and matter non-standard neutrino interactions at DUNE,” (2016), 1606.08851.

[23] A. de Gouv  a and K. J. Kelly, “Non-standard Neutrino Interactions at DUNE,” *Nucl. Phys.* **B908**, 318 (2016), 1511.05562.

[24] F. Capozzi, E. Lisi, A. Marrone, D. Montanino, and A. Palazzo, “Neutrino masses and mixings: Status of known and unknown 3ν parameters,” *Nucl. Phys.* **B908**, 218 (2016), 1601.07777.

[25] M. C. Gonzalez-Garcia, M. Maltoni, and T. Schwetz, “Global Analyses of Neutrino Oscillation Experiments,” *Nucl. Phys.* **B908**, 199 (2016), 1512.06856.

[26] D. V. Forero, M. Tortola, and J. W. F. Valle, “Neutrino oscillations refitted,” *Phys. Rev.* **D90**, 093006 (2014), 1405.7540.

[27] P. Vahle (2016), talk given at the Neutrino 2016 Conference, July 4-9, 2016, London, United Kingdom, <http://neutrino2016.iopconfs.org/home>.

[28] R. N. Mohapatra and A. Y. Smirnov, “Neutrino Mass and New Physics,” *Ann. Rev. Nucl. Part. Sci.* **56**, 569 (2006), [hep-ph/0603118](#).

[29] C. H. Albright and M.-C. Chen, “Model Predictions for Neutrino Oscillation Parameters,” *Phys. Rev.* **D74**, 113006 (2006), [hep-ph/0608137](#).

[30] G. Altarelli and F. Feruglio, “Discrete Flavor Symmetries and Models of Neutrino Mixing,” *Rev. Mod. Phys.* **82**, 2701 (2010), 1002.0211.

[31] S. F. King, A. Merle, S. Morisi, Y. Shimizu, and M. Tanimoto, “Neutrino Mass and Mixing: from Theory to Experiment,” *New J. Phys.* **16**, 045018 (2014), 1402.4271.

[32] S. F. King, “Models of Neutrino Mass, Mixing and CP Violation,” *J. Phys.* **G42**, 123001 (2015), 1510.02091.

[33] R. Acciari et al. (DUNE), “Long-Baseline Neutrino Facility (LBNF) and Deep Underground Neutrino Experiment (DUNE),” (2016), 1601.05471.

[34] R. Acciari et al. (DUNE), “Long-Baseline Neutrino Facility (LBNF) and Deep Underground Neutrino Experiment (DUNE),” (2015), 1512.06148.

[35] J. Strait et al. (DUNE), “Long-Baseline Neutrino Facility (LBNF) and Deep Underground Neutrino Experiment (DUNE),” (2016), 1601.05823.

[36] R. Acciari et al. (DUNE), “Long-Baseline Neutrino Facility (LBNF) and Deep Underground Neutrino Experiment (DUNE),” (2016), 1601.02984.

[37] C. Adams et al. (LBNE), “The Long-Baseline Neutrino Experiment: Exploring Fundamental Symmetries of the Universe,” (2013), 1307.7335.

[38] P. Bakhti and A. N. Khan, “Sensitivities to charged-current nonstandard neutrino interactions at DUNE,” (2016), 1607.00065.

[39] G. Mitsuka et al. (Super-Kamiokande), “Study of Non-Standard Neutrino Interactions with Atmospheric Neutrino Data in Super-Kamiokande

I and II," Phys. Rev. **D84**, 113008 (2011), [1109.1889](#).

[40] M. C. Gonzalez-Garcia and M. Maltoni, "Determination of matter potential from global analysis of neutrino oscillation data," JHEP **09**, 152 (2013), [1307.3092](#).

[41] T. Kikuchi, H. Minakata, and S. Uchinami, "Perturbation Theory of Neutrino Oscillation with Nonstandard Neutrino Interactions," JHEP **0903**, 114 (2009), [0809.3312](#).

[42] N. Klop and A. Palazzo, "Imprints of CP violation induced by sterile neutrinos in T2K data," Phys. Rev. **D91**, 073017 (2015), [1412.7524](#).

[43] V. Barger, D. Marfatia, and K. Whisnant, "Breaking eight fold degeneracies in neutrino CP violation, mixing, and mass hierarchy," Phys. Rev. **D65**, 073023 (2002), [hep-ph/0112119](#).

[44] S. K. Agarwalla, S. S. Chatterjee, A. Dasgupta, and A. Palazzo, "Discovery Potential of T2K and NOvA in the Presence of a Light Sterile Neutrino," JHEP **02**, 111 (2016), [1601.05995](#).

[45] S. K. Agarwalla, S. S. Chatterjee, and A. Palazzo, "Physics Reach of DUNE with a Light Sterile Neutrino," (2016), [1603.03759](#).

[46] P. Coloma and T. Schwetz, "Generalized mass ordering degeneracy in neutrino oscillation experiments," (2016), [1604.05772](#).

[47] S. K. Agarwalla, T. Li, and A. Rubbia, "An Incremental approach to unravel the neutrino mass hierarchy and CP violation with a long-baseline Superbeam for large θ_{13} ," JHEP **1205**, 154 (2012), [1109.6526](#).

[48] Mary Bishai, private communication (2012).

[49] P. Huber, M. Lindner, and W. Winter, "Simulation of long-baseline neutrino oscillation experiments with GLoBES (General Long Baseline Experiment Simulator)," Comput.Phys.Commun. **167**, 195 (2005), [hep-ph/0407333](#).

[50] P. Huber, J. Kopp, M. Lindner, M. Rolinec, and W. Winter, "New features in the simulation of neutrino oscillation experiments with GLoBES 3.0: General Long Baseline Experiment Simulator," Comput.Phys.Commun. **177**, 432 (2007), [hep-ph/0701187](#).

[51] A. M. Dziewonski and D. L. Anderson, "Preliminary reference earth model," Physics of the Earth and Planetary Interiors **25**, 297 (1981).

[52] P. Huber, M. Lindner, and W. Winter, "Superbeams versus neutrino factories," Nucl.Phys. **B645**, 3 (2002), [hep-ph/0204352](#).

[53] G. L. Fogli, E. Lisi, A. Marrone, D. Montanino, and A. Palazzo, "Getting the most from the statistical analysis of solar neutrino oscillations," Phys. Rev. **D66**, 053010 (2002), [hep-ph/0206162](#).

[54] M. Blennow, P. Coloma, P. Huber, and T. Schwetz, "Quantifying the sensitivity of oscillation experiments to the neutrino mass ordering," JHEP **03**, 028 (2014), [1311.1822](#).

[55] M. Gonzalez-Garcia, M. Maltoni, and J. Salvado, "Testing matter effects in propagation of atmospheric and long-baseline neutrinos," JHEP **1105**, 075 (2011), [1103.4365](#).

[56] P. Adamson et al. (MINOS), "Search for flavor-changing non-standard neutrino interactions by MINOS," Phys. Rev. **D88**, 072011 (2013), [1303.5314](#).

[57] S. K. Agarwalla, S. S. Chatterjee, and A. Palazzo, "Octant of θ_{23} in danger with a light sterile neutrino," (2016), [1605.04299](#).

[58] O. G. Miranda, M. Tortola, and J. W. F. Valle, "New ambiguity in probing CP violation in neutrino oscillations," (2016), [1604.05690](#).